

Deposition of ultrathin rare-earth doped Y_2O_3 phosphor films on alumina nanoparticles

Jie Lian¹, L Yang², X Y Chen³, G K Liu³, L M Wang¹, R C Ewing¹
and Donglu Shi^{2,4}

¹ Departments of Geological Sciences, Nuclear Engineering and Radiological Sciences and Materials Science and Engineering, University of Michigan, Ann Arbor, MI 48109, USA

² Department of Materials Science and Engineering, University of Cincinnati, Cincinnati, OH 45221-0012, USA

³ Chemistry Division, Argonne National Laboratory, Argonne, IL 60439, USA

E-mail: shid@email.uc.edu

Received 11 October 2005, in final form 16 January 2006

Published 10 February 2006

Online at stacks.iop.org/Nano/17/1351

Abstract

Ultrathin films of Eu^{3+} doped Y_2O_3 were deposited onto alumina nanoparticles using a unique solution synthesis method. The surface structure, composition, and morphology of the thin films deposited were analysed using high resolution transmission electron microscopy (TEM) and high angle annular dark field scanning TEM imaging and energy dispersive x-ray measurements. The films deposited were extremely thin, on the order of 3–5 nm, and uniformly covered all the alumina nanoparticles. X-ray diffraction was used to investigate the phases and structures of the thin films deposited. At the heat treatment temperature of 600 °C, cubic Y_2O_3 nanocrystals were found in the film while as-coated layers exhibited mainly amorphous features. As the heat treatment temperature increased to 750 °C, the amorphous thin film became well crystallized. Optical properties of Eu^{3+} doped Y_2O_3 films were characterized by fluorescence spectroscopy. Strong photoluminescence was observed in the sample annealed at 750 °C, from the fluorescence of Eu^{3+} ions in a well-crystallized film, consistent with the x-ray diffraction and TEM observations.

1. Introduction

Nanostructured materials, especially those containing optically active rare-earth elements, have been studied intensively due to their unexpected properties. These materials find important applications in lasers, optical amplifiers, and optical display phosphors. Particular interest is focused on the effects of particle dimensions, compositions, surface structures and morphologies on the optical properties. From the viewpoint of fundamental studies, the nanostructure related physical phenomena include the dependence of the electron–phonon interaction strength on the particle size [1], surface quenching [2], modification in transition intensity and fluo-

rescence lifetime [3], single-ion luminescence [4], restricted phonon relaxation and anomalous thermalization [5, 6]. These behaviours are all related to structural characteristics of the nanoparticles and distribution of the emission centres within them. Therefore, it is critical to develop new nanostructures, including new surface structures, which allow us to tune the physical properties by controlling the structure. A few experiments have been conducted on nanosurface structures in the study of nanophosphors [7]. Deposition of ultrathin rare-earth doped oxide films on nanoparticles may serve as a sensitive probe for the local environment. Such a new surface structure will be of significance in both fundamental research and engineering applications.

Eu^{3+} doped cubic Y_2O_3 crystals are red phosphors, commonly used in optical display and lighting applications.

⁴ Author to whom any correspondence should be addressed.

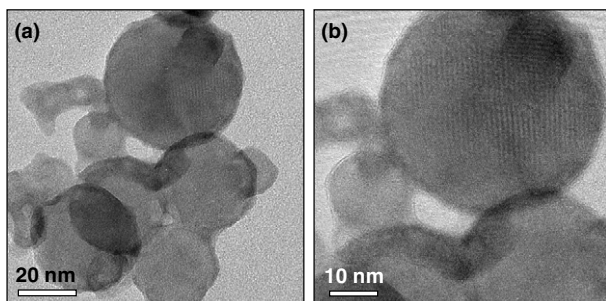


Figure 1. Bright field TEM images showing the coating layers on the surfaces of Al_2O_3 nanoparticles annealed at 600°C .

Nanosized particles of $\text{Eu}:\text{Y}_2\text{O}_3$ prepared by gas phase condensation or wet chemical methods have been extensively studied [8, 9], but few investigations have dealt with the deposition of ultrathin phosphor films on the surfaces of nanoparticles. In this paper, we present experimental results on the deposition of Eu^{3+} doped cubic Y_2O_3 ultrathin films on alumina nanoparticles. The films deposited were characterized using high resolution transmission electron microscopy (HRTEM) and high angle annual dark field (HAADF) STEM imaging. The optical behaviours of the surface functionalized nanoparticles were studied by fluorescence spectroscopy.

2. Experimental details

The deposition of Eu^{3+} doped cubic Y_2O_3 phosphors on alumina nanoparticles was achieved by forced hydrolysis as follows. 0.5 g of Al_2O_3 nanoparticles with diameters of 27–56 nm were dispersed in 300 ml deionized water and sonicated for 0.5 h; this was followed by 0.5 h of stabilization. Then certain amounts of YCl_3 (0.2 mol l^{-1}) and EuCl_3 (0.2 mol l^{-1}) were added. While being sonicated, the solution was titrated with ammonia (1 mol l^{-1}) at a speed of 1 ml min^{-1} . Vibration and titration were stopped before the pH reached the IEP of yttria (i.e., slightly above 8, at which point the solution was opaque but no aggregates formed) to allow incubation for more than 2 h. The process was then continued to fully deposit the anions. All these steps were carried out in ambient conditions. The precipitates were separated and collected by centrifuging and rinsing, then dried and ground. The temperature of the drying process was strictly controlled in the sequence by first increasing to 300°C from room temperature at a rate of 20°C h^{-1} and then holding at 300°C for 3 h, and finally lowering to room temperature at a rate of 50°C h^{-1} . To investigate the crystallization and phase transition of the coated phosphors, the as-coated powders were annealed in a tube furnace at 600 and 750°C for 12 h, and this was followed by air quenching of the sample directly to room temperature.

The surface morphology and microstructure of the nanoparticles were studied using a JEOL 2010 F analytic transmission electron microscope. The TEM samples were prepared by dispersing nanopowders directly on holey carbon films supported with Cu grids. X-ray diffraction (XRD) studies were carried out on a Scintag theta–theta diffractometer using $\text{Cu K}\alpha$ radiation ($\lambda = 1.5406 \text{ \AA}$). Laser spectroscopic

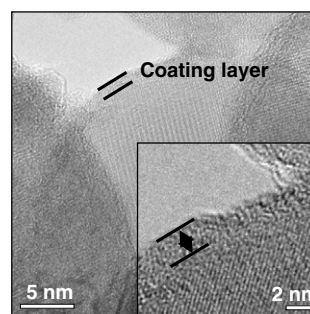


Figure 2. HRTEM images showing a uniform amorphous coating layer on the surface of alumina nanoparticles with the thickness of $\sim 3 \text{ nm}$.

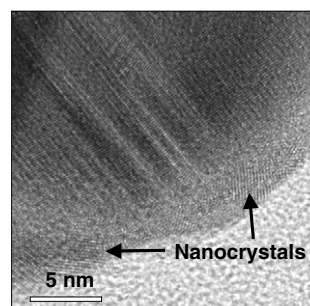


Figure 3. A HRTEM image showing the existence of nanocrystals in the coating layer annealed at 600°C .

experiments were conducted in order to study the optical behaviours of the surface functionalized nanoparticles.

3. Results and discussion

Figure 1 shows the bright field TEM images of Y_2O_3 coated alumina nanoparticles treated at 600°C . The alumina nanoparticles are spherical in shape, ranging between 20 and 60 nm in diameter. A coating layer is clearly evident on the outer surfaces of the alumina nanoparticles resulting from the solution deposition of Eu doped Y_2O_3 . The deposited film is uniform, entirely covering the alumina nanoparticles. HRTEM images (figure 2) indicate that the coating layer mainly exhibits amorphous structure, unlike the lattice images of the alumina substrate. Nanosized particles were also observed in the deposited film heat treated at 600°C , as evidenced by the HRTEM image (figure 3). Energy dispersive x-ray (EDX) spectra acquired from the coating layer show strong signals of Y and Eu, while the original nanoparticles contain only O and Al. The high angle annual dark field Z-contrast image (figure 4(a)) shows a contrast variation from the alumina substrate to the outer surface of nanoparticles. The bright contrast around the nanoparticles is attributed to the heavier elements of Y and Eu in the coating layer. Figure 4(b) shows the elemental profiles acquired by EDS line scanning in the STEM mode along the white line in figure 4(a) using an electron beam with the probe size of 0.5 nm. A compositional modulation is clearly evident across from the alumina nanoparticles to the coating layer, and the Y and

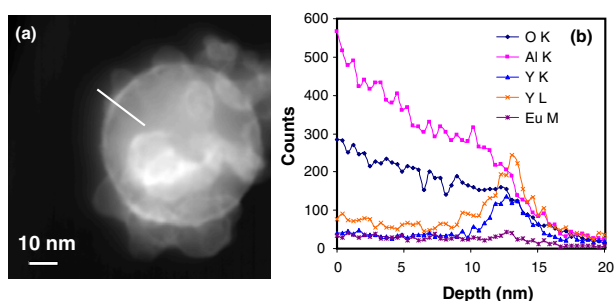


Figure 4. (a) A high angle annual dark field STEM (Z-contrast) image showing the coating layer on the surface of Al_2O_3 nanoparticles annealed at 600°C . The bright contrast around the nanoparticles is attributed to the heavier elements of Y and Eu in the coating layer. (b) The elemental profiles acquired along the solid line by STEM EDS line scanning.

Eu peaks at the elemental profile are located at the depth corresponding to the coating layer.

To further identify the phases and structures of the coating layers, XRD experiments were performed on these coated nanoparticles. As shown in figure 5(a), the XRD results for the as-coated sample show characteristic lines of Al_2O_3 phase and no evidence that the Y_2O_3 phase exists. This indicates that the coating layers of Y_2O_3 are amorphous in nature and most of them are actually in the form of yttrium oxyhydroxide (YOOH). As reported by Rao [6], the conversion of yttrium oxyhydroxide to oxide (or the crystallization) started at a temperature of 562°C for ultrafine Y_2O_3 particles prepared by sol-gel methods. Similarly, drying below 300°C during the preparation of the as-coated samples can only remove the adsorbed water molecules and not chemically bonded water. The XRD of the sample heated at 600°C (figure 5(b)) shows clearly the phases intermediate between the crystalline and amorphous phases, consistent with the HRTEM observations (figures 2 and 3). The crystalline phases include the alumina matrix, a small amount of cubic Y_2O_3 , and $\text{Y}_3\text{O}_4\text{Cl}$. The impurity phase of $\text{Y}_3\text{O}_4\text{Cl}$ could be formed accidentally during the co-deposition processes. These results indicate that coated layers of $\text{Eu}:\text{Y}_2\text{O}_3$ on Al_2O_3 nanoparticles using chemical deposition methods have nearly the same crystallization temperature as the particles prepared by the sol-gel method [6, 10]. When the as-coated sample was heated at 750°C for 12 h, the crystallization was mostly complete. As shown in figure 5(c), the XRD spectrum shows exclusive cubic Y_2O_3 crystal phase except the diffraction peaks from the matrix of the alumina particles.

The crystallization behaviours and phase transitions were studied in detail in our laser spectroscopic experiments. For the time-resolved fluorescence spectra, a pulsed dye laser with a tunable range from 510 to 550 nm, and an ultraviolet (UV) pulsed laser at 355 nm, were used to pump the samples. A boxcar integrator was used for the time-resolved fluorescence detection. For the boxcar, triggered by the pulsed laser signal, the sampling gate was delayed by 0.4 ms for selectively picking up the long-lived emission from the $^5\text{D}_0$ state of Eu^{3+} ions at crystalline lattice. The dye laser wavelength was tuned to excite the transition $^7\text{F}_0 \rightarrow ^5\text{D}_1$ in Eu^{3+} as a probe of crystalline lattices surrounding the Eu^{3+} ions.

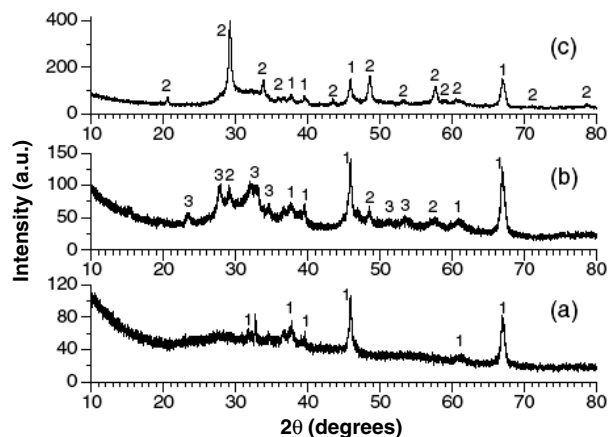


Figure 5. XRD spectra of (a) the as-grown sample; (b) the sample annealed at 600°C ; and (c) the sample annealed at 750°C . All the phases are well identified according to the standard data published by the International Centre for Diffraction Data (ICDD). Lines marked by numbers 1, 2 and 3 in the figure correspond respectively to Al_2O_3 , Y_2O_3 , $\text{Y}_3\text{O}_4\text{Cl}$ crystalline phases.

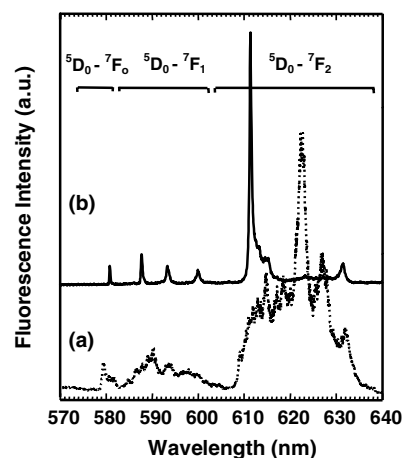


Figure 6. Emission spectra of (a) the sample annealed at 600°C , $\lambda_{\text{exc}} = 526.98$ nm, and (b) the sample annealed at 750°C , $\lambda_{\text{exc}} = 528.09$ nm. The intensity of the spectra was normalized to the same scale and all spectra were recorded at 4 K.

The fluorescence of Eu^{3+} ($^5\text{D}_0 \rightarrow ^7\text{F}_0$, $^7\text{F}_1$, and $^7\text{F}_2$) in the range of 570–640 nm was recorded, and the decay time of the Eu^{3+} fluorescence was measured using a digital storage oscilloscope. No Eu^{3+} fluorescence lines were recorded for the as-coated sample possibly due to non-radiative quenching by surface defects, whereas the sample annealed at 600°C (figure 6(a)) shows Eu^{3+} fluorescence lines that are much broader than those of Eu^{3+} in a crystalline phase. This result suggests that the Eu^{3+} ions are mainly located in an amorphous environment. In contrast, the narrow peaks in the emission spectrum of the samples annealed at 750°C (figure 6(b)) are from the fluorescence of Eu^{3+} ions in a crystalline lattice. The energy level structure of the spectrum is in good agreement with the previous works [11–14], suggesting a site of C_2 symmetry in the cubic Y_2O_3 crystal. The results of optical spectroscopic experiments suggest that the crystalline phase formed upon thermal annealing of the coated nanoparticles, which is consistent with the XRD and TEM results. Moreover,

the spectroscopic results confirm that the crystalline Y_2O_3 nanoparticles contain Eu^{3+} ions as luminescence centres.

The fluorescence lifetimes of Eu^{3+} ions in the coated and annealed nanoparticles have been measured at liquid helium and room temperature, respectively. The lifetime of the $^5\text{D}_0$ emitting state of Eu^{3+} in the samples heated at 750°C is 1.4 ms at 4 and 294 K, remarkably longer than the longest value of the bulk counterparts ever reported (1.1 ms) [15]. The longer lifetime of $^5\text{D}_0$ in the $\text{Eu}:\text{Y}_2\text{O}_3$ nanolayers is probably due to the non-solid medium surrounding the nanoparticles that changes the effective index of refraction, thus changing the radiative lifetime [3].

As discussed, the conventional phase diagram of the $\text{Y}_2\text{O}_3\text{--Al}_2\text{O}_3$ system indicates that bulk YAP melts incongruently and is unstable below 1600°C [14], but that may not be applicable in nanoscale thermodynamics. Note that the as-grown nanolayers of $\text{Eu}:\text{Y}_2\text{O}_3$ coated on the alumina nanoparticles may have extremely high surface energy, which could greatly lower the barrier for the reaction between the alumina cores and coating layers. Therefore, it may lead to non-equilibrium phase transitions by solid–solid diffusion processes. This barrier is closely related to the lattice binding energy, particle size, and morphology (surface effects). By controlling the composition of the starting materials, deposition process, and reaction kinetics of coated Y_2O_3 ultrathin films and Al_2O_3 substrates, it maybe possible to obtain a more homogeneous and pure phase of YAP (or YAG) crystalline films coated on alumina cores at relatively low temperatures, as compared to conventional solid state reaction for bulk samples. However, a fundamental understanding of the nanoscale chemical reaction and solid–solid diffusion processes has not been achieved yet, and thus needs further study.

4. Conclusions

Using a unique solution synthesis method, we have deposited an ultrathin Eu^{3+} doped Y_2O_3 film onto the surface of alumina nanoparticles. The HRTEM results show that the deposited films with the thickness of 3–5 nm uniformly cover the nanoparticles. Both the *Z*-contrast image and the EDX elemental profile indicate that the deposited films, resulting from the solution coating, contain mainly Eu and Y. XRD diffraction was used to investigate the phase compositions

of deposited films annealed at different temperatures. At 600°C , the deposited films mainly display amorphous features. However, a small content of crystalline Y_2O_3 nanoparticles exists in the coated film, leading to broad emissions in the visible light range. Strong photoluminescence occurs in the sample annealed at 750°C , from the fluorescence emission of Eu^{3+} ions in a well-crystallized film.

References

- [1] Hodak J H, Henglein A and Hartland G V 2000 *J. Chem. Phys.* **112** 5942
Hong K S, Meltzer R S, Bihari B, Williams D K and Tissue B M 1998 *J. Lumin.* **76/77** 234
- [2] Tissue B M 1998 *Chem. Mater.* **10** 2837
- [3] Meltzer R S, Feofilov S P, Tissue B and Yuan H B 1999 *Phys. Rev. B* **60** R14012
- [4] Bartko A P, Peyser L A, Dickson R M, Mehta A, Thundat T, Bhargava R and Barnes M D 2002 *Chem. Phys. Lett.* **358** 459
- [5] Meltzer R S and Hong K S 2000 *Phys. Rev. B* **61** 3396
Liu G K, Zhuang H Z and Chen X Y 2002 *Nano Lett.* **2** 535
Liu G K, Chen X Y, Zhuang H Z, Li S and Niedbala R S 2005 *J. Solid State Chem.* **178** 419
- [6] Rao R P 1996 *J. Electrochem. Soc.* **143** 189
Rao R P 1996 *Solid State Commun.* **99** 439
- [7] Zhang W W, Zhang W P, Xie P B, Yin M, Chen H T, Jing L, Zhang Y S, Lou L R and Xia S D 2003 *J. Colloid Interface Sci.* **262** 588
- [8] Chen X Y, Yang L, Cook R E, Skanthakumar S, Shi D and Liu G K 2003 *Nanotechnology* **14** 670
Chen X Y, Skanthakumar S, Liu G K, Yang L, Shi D, Lian J, Wang L M and Cook R E 2005 *Nanotechnology Focus* ed E V Dirote (New York: Nova Science) pp 141–73
- [9] Eilers H and Tissue B M 1996 *Chem. Phys. Lett.* **251** 74
Bihari B, Eilers H and Tissue B M 1997 *J. Lumin.* **75** 1
Williams D K, Bihari B, Tissue B M and McHale J M 1998 *J. Phys. Chem. B* **102** 916
- [10] Chang N C 1963 *J. Appl. Phys.* **34** 3500
Chang N C and Gruber J B 1964 *J. Chem. Phys.* **41** 3227
- [11] Shelby R M and Macfarlane R M 1981 *Phys. Rev. Lett.* **47** 1172
Erickson L E and Sharma K K 1981 *Phys. Rev. B* **24** 3697
Erickson L E 1986 *Phys. Rev. B* **34** 36
- [12] Koningstein J A 1964 *Phys. Rev.* **136** A717
Asano M and Koningstein J A 1979 *Chem. Phys.* **42** 369
- [13] Liu S and Su Q 1997 *J. Alloys Compounds* **255** 102
- [14] Gross H, Neukum J, Heber J, Mateika D and Xiao T 1993 *Phys. Rev. B* **48** 9264
- [15] Bondar I A, Koroleva L N and Bezruk E T 1984 *Inorg. Mater.* **20** 214